

# Effects of the Polydispersity on Rheological Properties of Entangled Polystyrene Solutions

Xiangnan Ye and Tam Sridhar\*

Department of Chemical Engineering, Monash University, Clayton VIC3800, Australia

Received February 22, 2004; Revised Manuscript Received February 1, 2005

**ABSTRACT:** Previous studies on extensional properties of entangled solutions have mainly dealt with monodisperse polymers. To investigate the effect of polydispersity on rheological properties of entangled polystyrene solutions, a polydisperse blend with an average molecular weight of  $2.65 \times 10^6$  was made by mixing 18 components of nearly monodisperse polystyrene. The effect of polydispersity is illustrated by comparing the rheological behavior of this blend with that of a solution of monodisperse polymer with the same average molecular weight and at the same concentration. Shear, small-amplitude sinusoidal flow, step strain in shear, and uniaxial extension are used in this study. The multicomponent system has a much broader relaxation spectrum and a slightly smaller zero-shear-rate viscosity than the solution of monodisperse polymer. The shear thinning behavior of the two solutions are very similar except that the polydisperse system shows an earlier onset of shear thinning. In step strain experiments, the polydisperse system requires a larger time for the completion of the Rouse equilibration process while the damping function is not dissimilar. These differences are attributed to the high molecular weight components in the polydisperse system. As anticipated, the differences in extensional flow are far more dramatic, reinforcing the sensitivity of this particular measurement to the molecular weight distribution. The predictions of the single mode (“toy” model) version of the Mead–Larson–Doi model are compared with the data. The parameters in this model are obtained using a separate set of experiments with monodisperse polymers to develop appropriate scaling relationships. The model provides near-quantitative predictions of these results.

## I. Introduction

It is well-known that rheological properties of polymeric fluids are profoundly influenced by the molecular weight distribution (MWD). The simplest case of a wide MWD is the binary blend of linear polymers, which has been well studied experimentally and theoretically.<sup>1–5</sup> During the past decade, the effect of polydispersity has received some attention.<sup>6,7</sup> Most of these investigations have mainly focused on the linear viscoelastic response, with only a very few of them dealing with extensional flows.<sup>8</sup> The development of the filament stretching technique<sup>9,10</sup> permits one to investigate the rheological behavior of polymer solutions in uniaxial extensional flows and gives us an opportunity to address the impact of polydispersity in extensional flows. A recent review of this technique and its applications can be found elsewhere.<sup>11</sup>

Several blending rules have been developed to capture the effect of the polydispersity on both binary blends and polydisperse blends with a wide MWD. Among these, the Ninomiya blending rule<sup>12</sup> was found to be successful in some binary blends,<sup>3</sup> while the quadratic blending rule<sup>13</sup> has been successfully applied for polydisperse entangled systems.<sup>6,7,14</sup> Entangled systems are typically studied within the framework of the reptation theory<sup>15</sup> which envisages a chain in a melt to be confined within a tube of constraints. In the original theory, reptation was the only mechanism for stress relaxation. Several additional mechanisms such as contour length fluctuations (CLF), chain stretching (CS), and constraint release (in the form of tube renewal or double reptation) have been incorporated into the original Doi–Edwards model<sup>15</sup> and provide a basis for understanding the interaction between polymer chains in polydisperse systems. Models incorporating reptation along with

these relaxation mechanisms are available. A simplified single-mode version of the Mead–Larson–Doi (MLD) model<sup>16</sup> was developed to predict the rheological behavior of polydisperse systems in fast flows. This so-called “toy” MLD model was found to be successful for the case of binary blends of entangled polymer solutions in the shear<sup>17</sup> and the extensional flow.<sup>18</sup> In addition, Pattamaprom and Larson also applied this model to polydisperse melts and were able to predict the steady-state viscosity.<sup>19</sup> This paper tests the “toy” MLD model further for a general polydisperse solution subjected to extensional flow. One monodisperse polystyrene entangled solution and a tailored polydisperse polystyrene solution, which is a mixture of 18 nearly monodisperse components, with same average molecular weight and concentration are used to examine the impact of polydispersity on rheology. The paper is organized as follows. Section II describes the experimental procedure in detail, and section III provides an outline of the “toy” MLD model which provides the theoretical framework. The results from the experiments are presented and discussed in section IV. Section V concludes the paper by summarizing the findings.

## II. Experiments

### A. Solution Preparation and sample Characterization.

One way to obtain a well-characterized wide MWD sample is by mixing several nearly monodisperse polymers, each of which is assumed to have a log-normal (LN) distribution given by

$$\psi(M) = \frac{1}{\delta\sqrt{2\pi}} \frac{1}{M} \exp\left(-\frac{1}{2\delta^2}(\ln M - \ln m_0)^2\right) \quad (1)$$

where  $\psi$  is the probability density;  $m_0 = M_w/\sqrt{p}$  characterizes the peak value of the MWD, and  $\delta$  is the standard deviation that specifies the polydispersity  $p$ . In addition, it is assumed

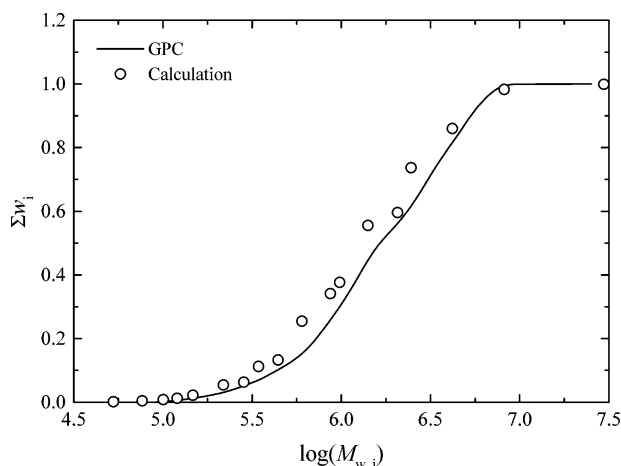


**Figure 1.** Comparison of cumulative weight fraction as a function of molecular weight for calculation and GPC result for P1.

**Table 1. Composition of the Polydisperse Mixture of Polystyrene Standards, the P1 Solution**

no.	$M_{w,i}$	polydispersity $P_i$	weight fraction $w_i$	$w_i \times M_{w,i}/M_e^{\text{soln}}$
1	52 630	1.03	0.002	$4.46 \times 10^{-4}$
2	76 500	1.04	0.003	$9.76 \times 10^{-4}$
3	100 400	1.03	0.004	$1.71 \times 10^{-3}$
4	120 200	1.04	0.004	$2.04 \times 10^{-3}$
5	147 000	1.03	0.010	$6.00 \times 10^{-3}$
6	218 000	1.05	0.032	$2.97 \times 10^{-2}$
7	284 000	1.05	0.009	$1.09 \times 10^{-2}$
8	343 700	1.05	0.049	$6.98 \times 10^{-2}$
9	442 000	1.04	0.020	$3.76 \times 10^{-2}$
10	601 200	1.07	0.122	$3.12 \times 10^{-1}$
11	868 800	1.05	0.087	$3.22 \times 10^{-1}$
12	978 000	1.04	0.035	$1.46 \times 10^{-1}$
13	1 410 000	1.05	0.179	1.07
14	2 068 000	1.04	0.041	0.36
15	2 461 000	1.04	0.141	1.48
16	4 196 000	1.05	0.123	2.20
17	8 186 000	1.11	0.123	4.28
18	29 640 000	1.3	0.016	2.02

that the resulting polydisperse mixture also has a LN distribution. Thus, for a desired MWD, the weight fractions of each component can be obtained by equating the sum of probability density contributions of each component to the desired probability density of the polydisperse mixture. The molecular weight for each component is so chosen to cover the range of molecular weight evenly. This procedure enables one to obtain a polydisperse polymer with a particular molecular weight and a specified polydispersity. In this work, we design a polydisperse mixture (P1) utilizing polystyrene standards with target molecular weight of  $2.89 \times 10^6$  and polydispersity of 3.5. The number of components is chosen to make the distribution of final mixture as smooth as possible. For practical purpose, however, the number of components is to be kept small. Thus, 18 components are required to obtain such a polydisperse mixture, with compositions shown in Table 1. One can also examine the fraction of the total number of entanglements  $w_i \times M_{w,i}/M_e^{\text{soln}}$  contributed by each component. Clearly, no. 13–18 components are dominant and therefore referred to as the major components from here onward.

Characterization of the resulting P1 mixture was also carried out by gel permeation chromatography (GPC). Figure 1 shows the cumulative weight fraction as a function of molecular weight. The GPC result is in good agreement with the desired distribution. The measured average molecular weight and polydispersity are  $2.65 \times 10^6$  and 3.2, respectively, for the P1 mixture, which slightly less than the design values.

A solution of P1 was prepared by dissolving the appropriate quantities of the polystyrene standards in tricresyl phosphate

(TCP) to make a 7% solution. Methylene chloride was used as a cosolvent. All of the polystyrene standards were purchased from either Polymer Source, Inc. (Canada), or Polymer Laboratories (UK) and used as received. Details of solution preparation can be found elsewhere.<sup>6,17,20</sup> A monodisperse polystyrene solution, L289, with molecular weight of  $2.89 \times 10^6$  and polydispersity of 1.08, also having a concentration of 7%, was kindly provided by Prof. Larson at University of Michigan.

**B. Rheological Measurements.** Shear and dynamic experiments were conducted with a strain-controlled rheometer, rheometrics fluid spectrometer (RFS II). A cone and plate geometry with diameter of 50 mm and a cone angle of 0.04 rad was used in this work. All measurements were conducted at 21 °C. The extensional viscosity was measured by the filament stretching rheometer. Details of the technique are available elsewhere.<sup>21</sup> Over a wide range of deformation rates, this device provides reproducible and reliable results for both dilute and concentrated solutions. Steady state for these solutions is obtained beyond a strain of 4.

### III. Theoretical Background

**A. The “Toy” MLD Model.** For polydisperse systems, the stress tensor  $\sigma$  in the “toy” MLD model is expressed as the sum of each component’s contribution, i.e.

$$\sigma = 5 \sum_i w_i G_N^{0(\text{TM})} k_{s,i} (\lambda_i)^2 \mathbf{S}_i \quad (2)$$

where the subscripts  $i$  and  $j$  (in the following equations) denotes the contribution of the chain  $i$  and  $j$  in the blends, respectively. The symbols  $w$  is the weight fraction and  $G_N^0$  is the plateau modulus and independent of molecular weight. However,  $G_N^{0(\text{TM})}$  is the model-dependent plateau modulus which incorporates the effect of CLF. As a result, it is dependent on molecular weight. The nonlinear spring coefficient,  $k_s$ , can be approximated by the normalized Padé inverse Langevin function as

$$k_s = \frac{(3 - \alpha^2)(1 - \beta^2)}{(1 - \alpha^2)(3 - \beta^2)}$$

with  $\alpha$  being the ratio of the current tube length  $L_i$  to the maximum stretched length  $L_{\text{ax}}$  and  $\beta$  being the ratio of the equilibrium length of a segment  $L_{\text{eq}}$  to  $L_{\text{ax}}$ .  $\lambda_i$  is the stretch ratio given by  $\lambda_i = L_i/L_{\text{eq}}$ . Clearly,  $\beta$  is independent of molecular weight and equals 0.056 for a 7% polystyrene solution. As mentioned in an earlier work,<sup>18</sup> a higher value of  $\beta$  ( $\beta = 0.12$ ) significantly improves the “toy” MLD model prediction of the steady-state extensional viscosity in the high strain rate region. Thus, this value is used in all calculations in this work. The orientation tensor  $\mathbf{S}_i$  is

$$\mathbf{S}_i = \sum_j w_j \int_{-\infty}^t \frac{dt'}{\tau_{ij}(t')} \exp\left(-\int_{t'}^t \frac{dt''}{\tau_{ij}(t'')}\right) \mathbf{Q}[\mathbf{E}(t, t')] \quad (3)$$

where  $\mathbf{E}(t, t')$  is the deformation gradient history and  $\mathbf{Q}[\mathbf{E}(t, t')]$  is the universal tensor which can be calculated using Currie’s approximation<sup>22</sup>

$$\mathbf{Q} \approx \left(\frac{1}{J-1}\right) \mathbf{B} - \left(\frac{1}{(J-1)\sqrt{I_2+13/4}}\right) \mathbf{C} \quad (4a)$$

where  $\mathbf{B}$  and  $\mathbf{C}$  are Finger tensor and Cauchy tensor.  $I_1$  and  $I_2$  are the trace of the tensor  $\mathbf{B}$  and  $\mathbf{C}$ , respectively, and  $J \equiv I_1 + 2\sqrt{I_2+13/4}$ . Another approximation

**Table 2. The “Toy” MLD Model Parameters for Three Pure Monodisperse Solutions**

	L289	L384	L842
mol wt	$2.89 \times 10^6$	$3.84 \times 10^6$	$8.42 \times 10^6$
$G_N^{0(TM)}$ (Pa)	349.6	384.3	480.4
$\tau_d^{(TM)}$ (s)	9.4	23.1	189.6
$\tau_R^{(TM)}$ (s)	0.76	1.31	5.0

for  $\mathbf{Q}$  has also been proposed<sup>23</sup>

$$\mathbf{Q} \approx \frac{\mathbf{C}^{-1/2}}{\text{tr}(\mathbf{C}^{-1/2})} \quad (4b)$$

where “tr(...)” represents the trace operation. A comparison of (Q11–Q22) from these two approaches as a function of extension rate  $\dot{\epsilon}$  shows excellent agreement. In this work the Currie approximation is used.

The average relaxation time in eq 3,  $\tau_{ij}$ , is expressed as

$$\frac{1}{\tau_{ij}} = \frac{1}{\lambda_i^2 \tau_{d,i}} + \frac{1}{\lambda_i} \left( \mathbf{K} : \mathbf{S}_j - \frac{\dot{\lambda}_j}{\lambda_j} + \frac{1}{\lambda_j^2 \tau_{d,j}} \right) \quad (5)$$

where  $\tau_d$  is the reptation time and  $\mathbf{K}$  is the velocity gradient tensor. The time derivative of stretch ratio  $\lambda$  can be calculated from the differential equation

$$\dot{\lambda}_i = \lambda_i \mathbf{K} : \mathbf{S}_i - \frac{k_{s,i}(\lambda_i)}{\tau_{R,i}} (\lambda_i - 1) - \frac{1}{2} (\lambda_i - 1) \sum_j w_j \left( \mathbf{K} : \mathbf{S}_j - \frac{\dot{\lambda}_j}{\lambda_j} + \frac{1}{\lambda_j^2 \tau_{d,j}} \right) \quad (6)$$

where  $\tau_R$  is the Rouse time.

Note that both convective constraint release (CCR)<sup>24,25</sup> and the chain stretching (CS)<sup>26</sup> have been incorporated in this model. CCR enhances the relaxation in eq 5 (first two terms in brackets) and affects the chain stretching through similar terms in eq 6. The extent of the impact of CCR on eqs 5 and 6 is controlled by the switch function  $1/\lambda_i$ . The effect of contour length fluctuations (CLF) can be indirectly introduced through appropriate changes to the model parameters.<sup>18</sup>

**B. Estimation of the “Toy” MLD model Parameters.** Before applying the “toy” MLD model to predict the rheological behavior of the P1 solution, we briefly demonstrate the procedure for obtaining the model parameters as follows. The parameters are estimated by the method developed by Ye et al.<sup>18</sup>

The molecular weight between entanglements for 7% polystyrene solution was found to be  $2.35 \times 10^5$  according to the scaling of  $M_e^{\text{soln}}$  with concentration.<sup>18,27</sup> As a result, the plateau modulus and the number of entanglements for a 7% solution of polystyrene with an average molecular weight of  $2.89 \times 10^6$  (L289) are 619 Pa and 12.3, respectively. In addition, the Rouse time for a segment  $\tau_e$ , was obtained by fitting the experimental dynamic data by the modified Milner–McLeish model,<sup>28</sup> which is found to be  $5.0 \times 10^{-3}$  for 7% polystyrene solution.<sup>18</sup> Indeed, both  $M_e^{\text{soln}}$  and  $\tau_e$  are independent of the chain molecular weight.

The “toy” MLD model parameters are indicated by the superscript TM as  $G_{N,i}^{0(TM)}$ ,  $\tau_{d,i}^{(TM)}$ , and  $\tau_{R,i}^{(TM)}$  for each component of the polydisperse blend. Estimation of these

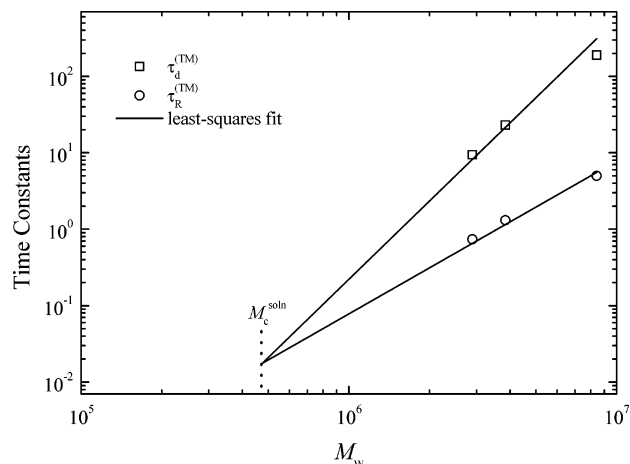


**Figure 2.** Dependence of the two time constants of the “toy” MLD model parameters,  $\tau_d^{(TM)}$  and  $\tau_R^{(TM)}$ , on the molecular weight. The solid lines are the least-squares fits and are expressed by eqs 8 and 9, respectively.

parameters for a monodisperse polymer was developed by Ye et al.<sup>18</sup> The method allows us to indirectly introduce the effect of contour length fluctuations into the “toy” MLD model. All these model parameters are dependent on molecular weight. The scaling of these parameters with molecular weight is evaluated using three monodisperse polystyrene solutions of the same concentration (see Table 2). Using these data, the relationship between the plateau modulus and molecular weight ( $M_{w,i}$ ) is

$$G_{N,i}^{0(TM)} = 4.4 M_{w,i}^{0.3} \quad (7)$$

For the two time constants, theory<sup>12</sup> predicts that for the molecular weight larger than the critical molecular weight ( $M_c^{\text{soln}} = 2M_e^{\text{soln}}$ ) the disengagement time with fluctuations and the Rouse time for each component follows a power law with exponents 3.4 and 2, respectively. We then have (see Figure 2)

$$\tau_{d,i}^{(TM)} = 8.8 \times 10^{-22} M_{w,i}^{3.4} \quad (8)$$

$$\tau_{R,i}^{(TM)} = 7.8 \times 10^{-14} M_{w,i}^2 \quad (9)$$

For components with the molecular weight smaller than the critical molecular weight  $M_c^{\text{soln}}$ , the disengagement time equals the Rouse time.<sup>19</sup> With these relationships, all model parameters are available (eqs 7–9), and the “toy” MLD model can be used to predict the properties of the polydisperse solution.

## IV. Results and Discussion

**A. Linear Viscoelasticity.** The measured dynamic storage modulus  $G'$  and loss modulus  $G''$  for both solutions at 21 °C are shown in Figure 3. Several differences can be observed due to effects of polydispersity. First, the L289 solution clearly shows the scale of  $G' \sim \omega^2$  and  $G'' \sim \omega$  in the low-frequency terminal region. For the P1 solution, however, this scaling is not apparent within the frequency range investigated. The terminal regime is relegated to lower frequencies due to the high molecular weight components in P1. Second, in the intermediate frequency region of  $0.1 \text{ rad/s} \leq \omega \leq 10 \text{ rad/s}$ , both  $G'$  and  $G''$  increase much more gradually with increasing frequency for the L289 solution than

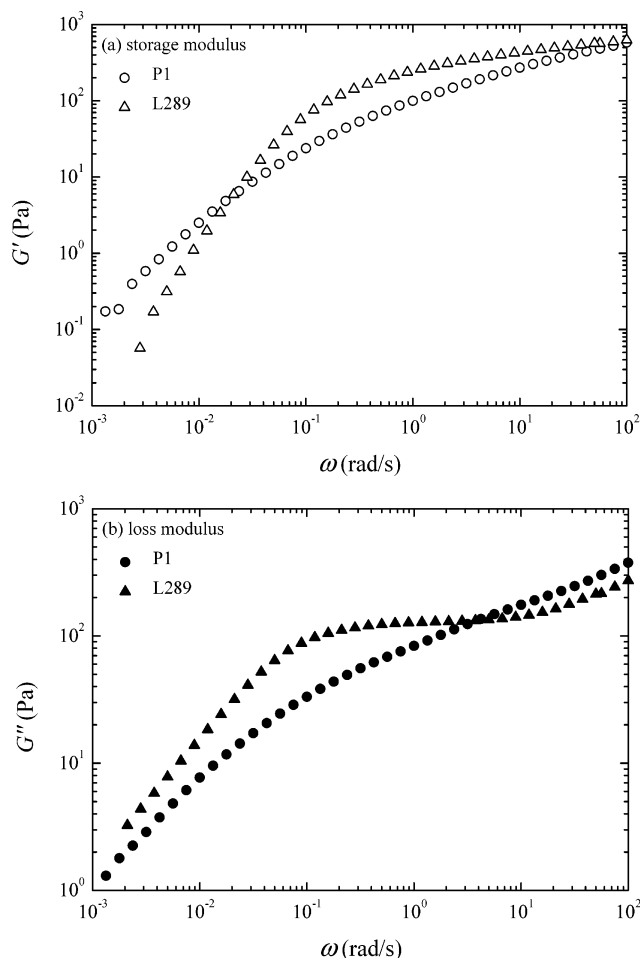


**Figure 3.** Comparison of (a) storage and (b) loss moduli for the P1 solution (circles) and the L289 solution (triangles) at 21 °C.

that for the P1 solution. This is to be expected since the contributions of each component to the storage modulus at the different frequencies is different. At these frequencies, the lower molecular weight components are in their terminal regime and their contribution to the modulus increases with frequency. The higher molecular weight components are in their plateau region and do not change with frequency. Third, both solutions show a similar frequency dependence of moduli in the high-frequency region, which indicates that the effect of polydispersity disappears due to the dominance of Rouse process in this region. However, since P1 has high molecular components and hence has higher value of  $\tau_R$ , the Rouse contribution will become significant at lower frequency for the P1 solution than that of the L289 solution.

Further evaluation of the linear viscoelastic data can be carried out by applying the double-reptation model,<sup>29</sup> where the stress relaxation modulus  $G(t)$  is expressed as

$$G(t) = G_N^0 \left[ \int_0^\infty w(M) \sqrt{F(t, M)} dM \right]^2 \quad (10)$$

where  $F(t, M)$  is the reduced relaxation function. A variety of expressions for the reduced relaxation function, such as the Tuminello step function,<sup>30</sup> the single-exponential function,<sup>13</sup> the des Cloizeaux function,<sup>31</sup> and the BSM empirical function,<sup>32</sup> have been used and compared with the experimental data for the com-

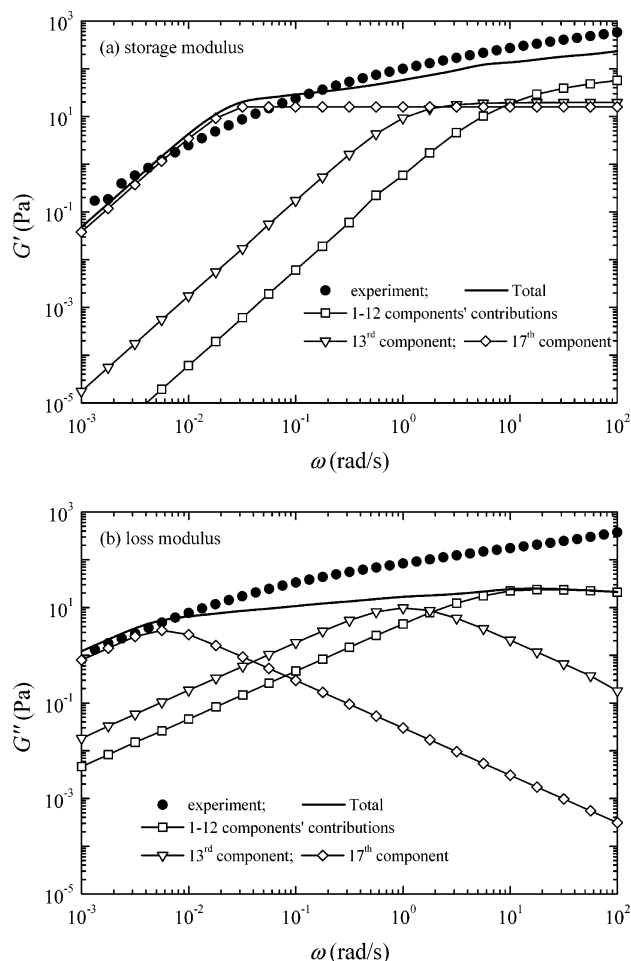


**Figure 4.** Comparison of the double-reptation model predictions of (a) storage and (b) loss moduli and the experimental data for the P1 solution. The contributions of some representative components are also shown for comparison.

mercial samples.<sup>6,7</sup> Among these, the single-exponential function is simple and accurate enough to generate good predictions. In this case

$$F(t, M) = \exp \left[ -\frac{t}{\tau(M)} \right] \quad (11)$$

where  $\tau(M)$  is the mean relaxation time of the component of molecular weight  $M$ , which is shown in eq 8. Figure 4 shows the comparison of the Fourier transform of  $G(t)$  using the single-exponential function and the experimental data for the P1 solution. The contributions to the moduli by some of the individual components are also shown for comparison. The high molecular weight components dominate in the low-frequency terminal region while the lower molecular weight component begin to become significant at higher frequencies. Indeed, this model is able to predict the linear viscoelasticity of polydisperse system fairly well, at least in the terminal regime.

**B. Nonlinear Viscoelasticity. B1. Step Strain Relaxation.** Extensive studies on the relaxation after a step shear strain have shown that the nonlinear relaxation modulus  $G(t, \gamma)$  can be separated into a time-dependent part and a strain-dependent part at long time  $t$ . That is,  $G(t, \gamma) = h(\gamma)G(t)$  with  $h(\gamma)$  being the shear damping function and  $G(t)$  being the linear relaxation modulus. Figure 5 shows the comparison of  $G(t, \gamma)$  for both solutions under a small shear strain of 5% and a



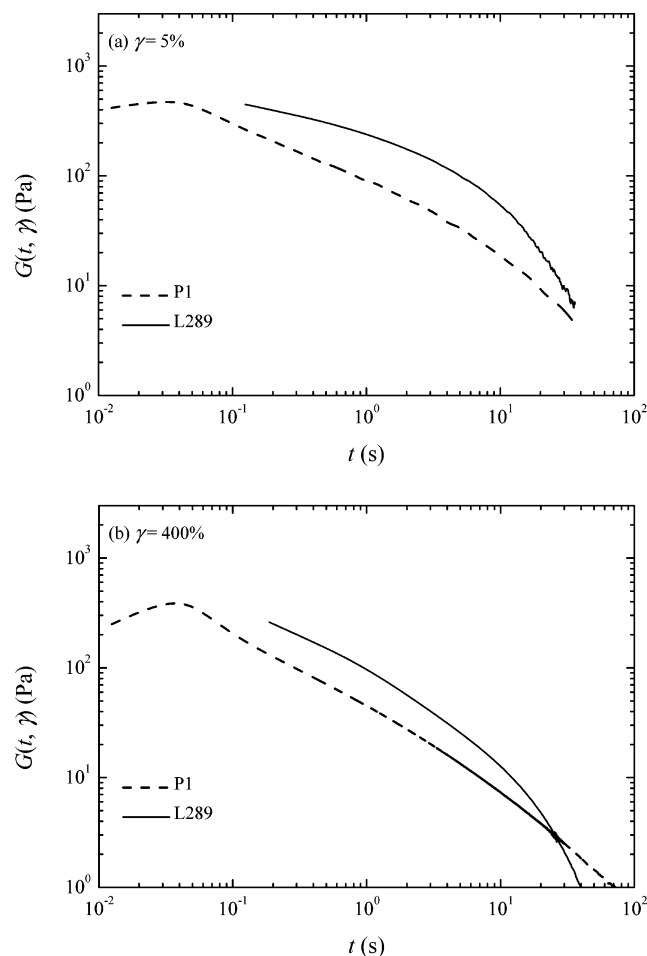


**Figure 5.** Comparison of the nonlinear relaxation modulus for both solutions under (a) shear strain of 5% and (b) shear strain of 400%.

relative high shear strain of 400%. Clearly, the P1 solution has much more gradual and broader relaxation spectrum than that of the L289 solution. It takes a longer time for the polydisperse solution to relax the stress. The retardation probably comes from interactions of polymer chains with various lengths in the polydisperse system.

Figure 6 shows the reduced modulus of  $G(t, \gamma)/h(\gamma)$  for both solutions under several shear strains. The arrow in the figure indicates the time  $\lambda_k$  beyond which the nonlinear relaxation modulus  $G(t, \gamma)$  can be factorized into a time-dependent part and a strain-dependent part. This is believed to be the time for Rouse equilibration after the step strain during which time the contour length retracts back to its equilibrium value. For the P1 solution, the collapse of the reduced modulus occurs at  $\lambda_k \approx 20$  s for all investigated shear strains, which is about 3 times greater than that of the L289 solution, where  $\lambda_k \approx 7$  s. The damping function is shown in Figure 7 for both solutions. The MLD model prediction is also shown for comparison. Note that the damping function for the polydisperse solution starts to deviate from that of the monodisperse solution at shear strain of 100%. This kind of deviation is similar to that of unentangled linear polymers,<sup>33</sup> which implies that the damping function is less pronounced for the P1 solution than for the L289 solution. This polydisperse solution behaves like an unentangled solution probably due to the fact that low molecular weight components behave as solvents.

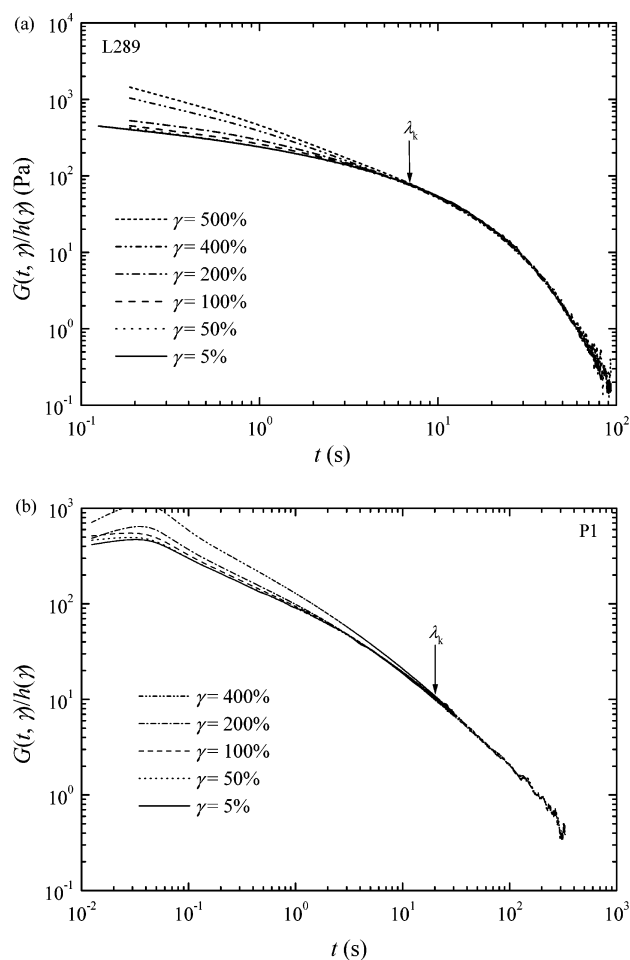


**Figure 6.** Reduced modulus for (a) the L289 solution and (b) the P1 solution under several shear strains.

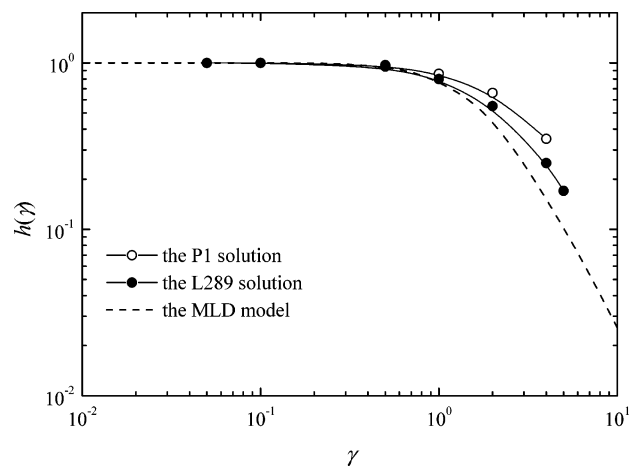


**Figure 7.** Comparison of the damping function for the L289 solution (filled circles), the P1 solution (open circles), and the "toy" MLD model prediction (the dashed line).

**B2. Steady Shear.** The startup of steady shear at two representative shear rates is shown in Figure 8 for L289 and P1. The "toy" MLD model predictions are also shown in solid lines for comparison. For the L289 solution, the "toy" MLD model can predict the shear viscosity growth over all time scale very well, except that a slight underprediction is observed near the peak of viscosity for  $2 \text{ s}^{-1}$ . For the P1 solution, however, the "toy" MLD model gives too much overpredictions on the shear viscosity for  $t > 1$  s in the case of shear rate of  $0.05 \text{ s}^{-1}$ , although it predicts very well the overall shear

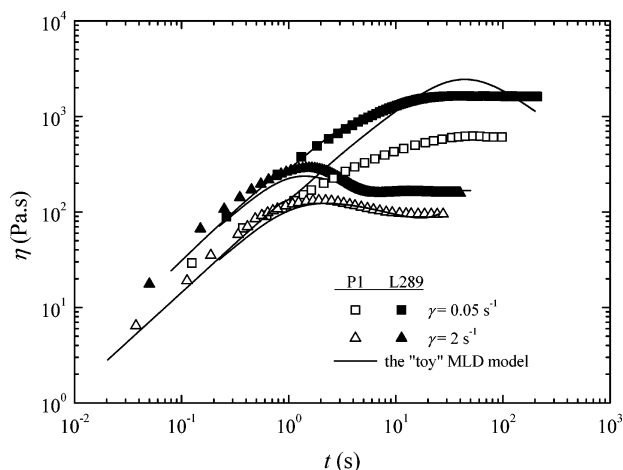


**Figure 8.** Comparison of the startup of shear viscosity at two shear rates for the L289 solution (filled symbols) and the P1 solution (open symbols) at shear rate of 0.05 and  $2 \text{ s}^{-1}$ . The solid lines are the "toy" MLD model predictions.

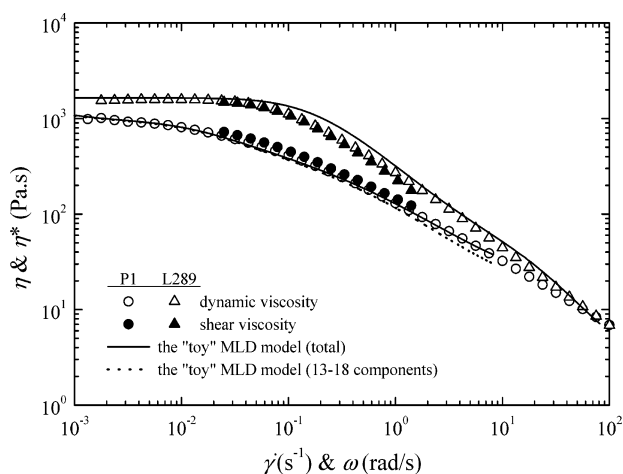


**Figure 9.** Comparison of the steady shear viscosity for the L289 solution (triangles), the P1 solution (circles) and the "toy" MLD model prediction (lines). The dynamic viscosity is also shown for both solutions in open symbols. The solid line is the prediction with all components' contributions, and the dotted line represents the major components' contributions.

viscosity for shear rate of  $2 \text{ s}^{-1}$  and the initial increase in shear viscosity for both solutions.

Figure 9 shows the comparison of steady shear viscosity for both solutions. The dynamic viscosities are also shown to demonstrate the validity of the empirical Cox–Merz rule.<sup>34</sup> While the viscosities are similar at low and high strain rates, there is a difference between these two solutions in the intermediate strain rates. The shear thinning for the P1 solution is much more gradual than the L289 solution. This is predominantly due to the higher polydispersity of the P1 solution. Note that the zero-shear-rate viscosity, taken from the plateau value of dynamic viscosity at low shear rate limit, is slightly smaller for the P1 solution. This is probably due to the presence of the low molecular weight components in P1, which act as a diluent.

The "toy" MLD model prediction for the P1 solution is also shown in Figure 9 for comparison. The solid line represents the contributions of all 18 components while the dotted line is the contribution of the major components (components 13–18). In principle, the contributions of those components with molecular weight less than  $M_c^{\text{soln}}$  should not included in eq 2. However, only a

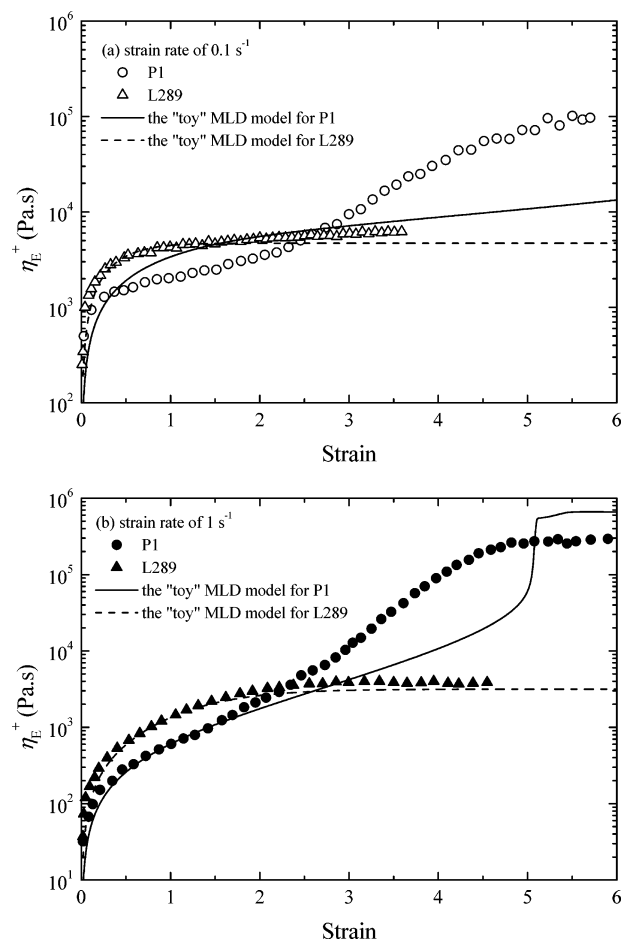


**Figure 10.** Comparison of the transient extensional viscosity for L289 (triangles) and P1 (circles) at strain rate of (a)  $0.1 \text{ s}^{-1}$  and (b)  $1 \text{ s}^{-1}$ . The lines are the "toy" MLD model predictions.

minor difference is observed when one considers contributions from all components. Clearly, the agreement with experimental data is excellent over the range of shear rates. In addition, it is observed that contributions mainly come from the major components. A slight deviation is only observed at the higher shear rates. In extensional flows, the dominance of the major components' contributions to total stress is expected to be even more significant and we will only consider their contributions.

**B3. Extensional Rheology.** The transient extension data are shown in Figure 10 by the extensional viscosity  $\eta_E^+$  as a function of strain at two representative strain rates. It is observed that the monodisperse solution reaches the steady-state earlier in both cases, at about two strain units for strain rate of  $1 \text{ s}^{-1}$ . For lower strain rate, the strain units required for L289 to get the steady state is even lower. In contrast, the polydisperse solution attains a steady state only after about five strain units. Moreover, the steady-state plateau of the P1 solution is much higher than that of the L289 solution in both cases studied, which indicates that the high molecular weight components are being stretched even at a strain rate of  $0.1 \text{ s}^{-1}$ . The "toy" MLD model predictions are also shown as a solid line in Figure 10 for comparison. In an earlier work,<sup>18</sup> the "toy" MLD model was shown to be capable of predicting the growth of extensional viscosity for monodisperse solutions. However, this work shows that it fails in predicting the transient extensional viscosity for polydisperse system at all strain

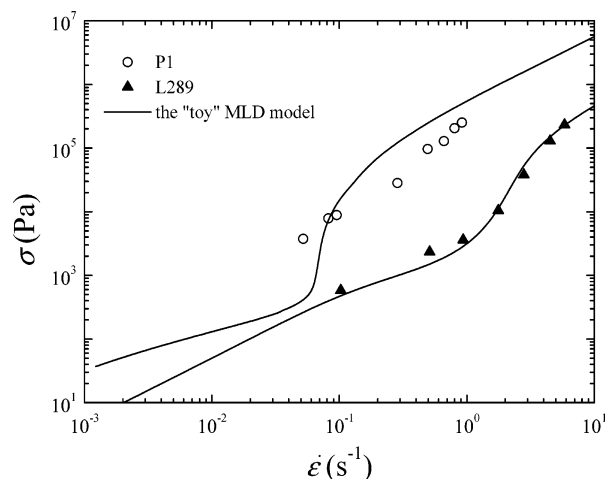


**Figure 11.** Comparison of the steady-state extensional stress for L289 (triangles) and P1 (circles). The lines are the “toy” MLD model predictions.

rates. For instance, the model prediction for P1 at strain rate of  $0.1 \text{ s}^{-1}$  does not reach a steady state at strain unit of 5, where the experimental data is already at steady plateau. Although it can predict the initial increase in extensional viscosity for P1 up to strain unit of 2 for strain rate of  $1 \text{ s}^{-1}$ , the “toy” MLD model underpredicts the extensional viscosity in the intermediate strain for both strain rates. Moreover, a sudden increase in the model prediction for P1 at strain rate of  $1 \text{ s}^{-1}$  is observed at strain unit of five, just before reaching the steady state, which does not occur in experiment.

The steady-state values of extensional stress are plotted against strain rate in Figure 11 for P1 and L289. Again, a huge difference can be observed between these two solutions. It is observed that P1 has much larger extensional stress than L289 over all strain rates studied. The difference can be up to two magnitudes at some strain rates. In addition, the onset of extension hardening is much lower for P1 than that for L289. This is probably due to the existence of the high molecular weight components in the polydisperse solution, where different polymer chains contribute at different time scales. To further examine the “toy” MLD model, its predictions on steady-state extensional stress are also shown in solid lines for both systems in Figure 11. Clearly, the model predicts the extensional stress very well for L289, while it can provide near quantitative predictions of extensional stress for P1. In other words, the model captures the overall trends in the extensional stress in the strain rate window investigated, although lack of experimental data at low strain rate region make the overall comparison unclear.

## V. Concluding Remarks

To study the effect of polydispersity on rheological properties, a polydisperse solution (P1) is prepared by mixing 18 nearly monodisperse polystyrene standards. The weight fractions of each component are designed so that the average molecular weight of the blend is  $2.89 \times 10^6$  and polydispersity is 3.5. Compared with a monodisperse polystyrene solution (L289) with same molecular weight at the same concentration, the polydisperse solution has a slightly smaller zero-shear-rate viscosity but exhibits a much larger extensional viscosity and a stronger strain hardening behavior over a wide

range of strain rates. The polydisperse solution is also found to have a more gradual and broader relaxation spectrum than that of the monodisperse solution.

To further examine the prediction of the “toy” MLD model for this polydisperse system, three monodisperse solutions of differing molecular weight but with the same concentration are used to develop model parameters and their scaling with molecular weight. The “toy” MLD model is found to provide an excellent prediction of the steady-state shear viscosity for this polydisperse solution. It is also able to predict the startup shear viscosity and transient extensional viscosity in the low strain region, but it fails to predict the overall viscosity growth under different strain rates. Moreover, the “toy” MLD model can also capture the steady-state behavior of extensional stress over the range of investigated strain rates.

**Acknowledgment.** The authors thank the Australian Research Council for a program grant. Useful comments by Professor Ron Larson are acknowledged.

## References and Notes

- (1) Graessley, W. W. The entanglement concept in polymer rheology. *Adv. Polym. Sci.* **1974**, *16*, 1–179.
- (2) Watanabe, H.; Sakamoto, T.; Kotaka, T. Viscoelastic properties of binary blends of narrow molecular weight distribution polystyrenes. 2. *Macromolecules* **1985**, *18*, 1008–1015.
- (3) Rubinstein, M.; Colby, R. H. Self-consistent theory of polydisperse entangled polymers: linear viscoelasticity of binary blends. *J. Chem. Phys.* **1988**, *89*, 5291–5306.
- (4) Juliani; Archer, L. A. Linear and nonlinear rheology of bidisperse polymer blends. *J. Rheol.* **2001**, *45*, 691–708.
- (5) Graessley, W. W.; Struglinski, M. J. Effects of polydispersity on the linear viscoelastic properties of entangled polymers. 2. comparison of viscosity and recoverable compliance with tube model predictions. *Macromolecules* **1986**, *19*, 1754–1760.
- (6) Wasserman, S. H.; Graessley, W. W. Effects of polydispersity on linear viscoelasticity in entangled polymer melts. *J. Rheol.* **1992**, *36*, 543–572.
- (7) Nobile, M. R.; Cocchini, F. Predictions of linear viscoelastic properties for polydisperse entangled polymers. *Rheol. Acta* **2000**, *39*, 152–162.
- (8) Munstedt, H. M. Dependence of the elongational behavior of polystyrene melts on molecular weight and molecular weight distribution. *J. Rheol.* **1980**, *24*, 847–867.
- (9) Tiratmadja, V.; Sridhar, T. A filament stretching device for measurement of extensional viscosity. *J. Rheol.* **1993**, *37*, 1081–1102.
- (10) Sridhar, T.; et al. Measurement of extensional viscosity of polymer solutions. *J. Non-Newtonian Fluid Mech.* **1991**, *40*, 271–280.
- (11) McKinley, G. H.; Sridhar, T. Filament stretching rheometry of complex fluids. *Annu. Rev. Fluid Mech.* **2002**, *34*, 375–415.
- (12) Ferry, J. D. *Viscoelastic Properties of Polymers*, 3rd ed.; Wiley: New York, 1980.
- (13) Tsenoglou, C. Molecular weight polydispersity effects on the viscoelasticity of entangled linear polymers. *Macromolecules* **1991**, *24*, 1726–1767.
- (14) Montfort, J. P.; Marin, G.; Mong, P. H. Molecular weight distribution dependence of the viscoelastic properties of linear polymers: the coupling of reptation and tube-renewal effects. *Macromolecules* **1986**, *19*, 1979–1988.
- (15) Doi, M.; Edwards, S. F. *The Theory of Polymer Dynamics*; Clarendon Press: Oxford, 1986.
- (16) Mead, D. W.; Larson, R. G.; Doi, M. A molecular theory for fast flows of entangled polymers. *Macromolecules* **1998**, *31*, 7895–7914.
- (17) Pattamaprom, C.; Larson, R. G. Constraint release effects in monodisperse and bidisperse polystyrenes in fast transient shearing flows. *Macromolecules* **2001**, *34*, 5229–5237.
- (18) Ye, X.; et al. Extensional properties of monodisperse and bidisperse polystyrene solutions. *J. Rheol.* **2003**, *47*, 443–468.

- (19) Pattamaprom, C.; Driscoll, J. J.; Larson, R. G. Nonlinear viscoelastic predictions of uniaxial-extensional viscosities of entangled polymers. *Macromol. Symp.* **2000**, *158*, 1–13.
- (20) Ye, X.; Sridhar, T. Shear and extensional properties of three-arm polystyrene solutions. *Macromolecules* **2001**, *34*, 8270–8277.
- (21) Bhattacharjee, P. K.; et al. Extensional rheometry of entangled solutions. *Macromolecules* **2002**, *35*, 10131–10148.
- (22) Currie, P. K. In *Proceeding of the Eight International Congress on Rheology*; Naples, Italy, 1980.
- (23) Marrucci, G.; Greco, F.; Ianniruberto, G. Simple strain measure for entangled polymers. *J. Rheol.* **2000**, *44*, 845–854.
- (24) Marrucci, G. Dynamics of entanglements: a nonlinear model consistent with the Cox-Merz rule. *J. Non-Newtonian Fluid Mech.* **1996**, *62*, 279–289.
- (25) Ianniruberto, G.; Marrucci, G. On compatibility of the Cox-Merz rule with the model of Doi and Edwards. *J. Non-Newtonian Fluid Mech.* **1996**, *65*, 241–246.
- (26) Marrucci, G.; Grizzuti, N. Fast flows of concentrated polymers: predictions of the tube model on chain stretching. *Gazz. Chim. Ital.* **1988**, *118*, 179–185.
- (27) de Gennes, P. G. *Scaling Concepts in Polymer Physics*; Cornell University Press: London, 1979.
- (28) Milner, S. T.; McLeish, T. C. B. Reptation and contour-length fluctuations in melts of linear polymers. *Phys. Rev. Lett.* **1998**, *81*, 725–728.
- (29) des Cloizeaux, J. Double reptation vs simple reptation in polymer melts. *J. Europhys. Lett.* **1998**, *5*, 437–442.
- (30) Tuminello, W. H. Molecular weight and molecular weight distribution from dynamic measurements of polymer melts. *Polym. Eng. Sci.* **1986**, *26*, 1339–1347.
- (31) des Cloizeaux, J. Relaxation and viscosity anomaly of melts made of entangled polymers: time dependent reptation. *Macromolecules* **1990**, *23*, 4678–4687.
- (32) Baumgaertel, M.; Schausberger, A.; Winter, H. H. Relaxation of polymers with linear flexible chains of uniform length. *Rheol. Acta* **1990**, *29*, 400–408.
- (33) Watanabe, H. Viscoelasticity and dynamics of entangled polymers. *Prog. Polym. Sci.* **1999**, *24*, 1253–1403.
- (34) Cox, W. P.; Merz, E. H. Correlation of dynamic and steady flow viscosities. *J. Polym. Sci.* **1958**, *28*, 619–622.

MA049642N